

High Energy WW Scattering at the LHC with the Matrix Element Method

A. Freitas¹ and J. S. Gainer^{2,3,4}

¹ Pittsburgh Particle-physics Astro-physics & Cosmology Center (PITT-PACC),
Department of Physics & Astronomy, University of Pittsburgh, Pittsburgh, PA 15260, USA

² High Energy Physics Division, Argonne National Laboratory, Argonne, IL 60439, USA

³ Department of Physics & Astronomy, Northwestern University, Evanston, IL 60208, USA

⁴ Physics Department, University of Florida, Gainesville, FL 32611, USA¹

NUHEP-TH/12-12, ANL-HEP-PR-12-104

Abstract

Perhaps the most important question in particle physics today is whether the boson with mass near 125 GeV discovered at the Large Hadron Collider (LHC) is the Higgs Boson of the Standard Model. Since a particularly important property of the Standard Model Higgs is its role in unitarizing $W_L W_L$ scattering, we study the ability of the LHC to probe this process in the case of same-sign W pair production. We find that the use of the Matrix Element Method increases the significance with which the Higgs sector can be probed in this channel. In particular, it allows one to distinguish between a light and heavy SM Higgs in this channel alone with a high degree of significance, as well as to set important limits in the parameter space of the Two Higgs Doublet Model and the Strongly-Interacting Light Higgs Model with less than 200 fb^{-1} at the 14 TeV LHC, thus providing crucial information about the putative Higgs boson's role in electroweak symmetry breaking.

¹Current address.

The mechanism of electroweak symmetry breaking (EWSB) can be tested most directly in high energy vector boson scattering. In fact, the tree-level amplitudes for scattering of longitudinally polarized $W_L W_L$, $Z_L Z_L$ and $W_L Z_L$ pairs involving only vector bosons grow unboundedly with energy until they violate the unitarity limit. This unphysical growth must be canceled by the dynamics of EWSB. For instance, in the Standard Model (SM), this is achieved by diagrams involving Higgs boson exchange. After the recent discovery of a Higgs-like resonance with a mass of 125–126 GeV [1] it will be essential to explicitly test whether this particle, other new physics, or a combination of the two are responsible for the unitarization of vector boson scattering.

In pp collisions, this question can be studied through processes of the type $pp \rightarrow jjV_1^*V_2^* \rightarrow jjV_1V_2$, where $V_i^{(*)}$ stands for a (off-shell) W - or Z -boson. Since these are four-body processes, the cross sections are small: even for $\sqrt{s} = 14$ TeV, the typical signal rates are $\mathcal{O}(\text{fb})$ or less. Furthermore, only a fraction of this rate is contributed by longitudinal vector bosons, so the analysis of such processes at the LHC is very challenging. Consequently, much effort has been invested in studying high energy vector boson scattering and the improvement of signal selection cuts [2–4]. Most of these papers focused on counting signal events or analyzing individual distributions (such as the VV invariant mass distribution). However, additional information may be gleaned from various angular correlations, which are sensitive to the details of the unitarity-restoring dynamics.

The Matrix Element Method (MEM) [5, 6] is a promising approach for comprehensively taking into account all information from an event and thus maximizing the sensitivity. It provides an algorithm for computing the likelihood that a given experimental event sample agrees with a theoretical model, using parton-level matrix elements and a set of input parameters. For each single event, with observed momenta $\mathbf{p}_i^{\text{vis}}$, the likelihood that it agrees with a given model and set of model parameters α is defined as

$$\mathcal{P}(\mathbf{p}_i^{\text{vis}}|\alpha) = \frac{1}{\sigma_\alpha} \sum_{k,l} \int dx_1 dx_2 \frac{f_k(x_1) f_l(x_2)}{2s x_1 x_2} \left[\prod_{j \in \text{inv.}} \int \frac{d^3 p_j}{(2\pi)^3 2E_j} \right] |\mathcal{M}_{kl}(p_i^{\text{vis}}, p_j; \alpha)|^2. \quad (1)$$

Here f_k and f_l are the parton distribution functions for the initial-state partons k and l , respectively, \mathcal{M}_{kl} is the theoretical matrix element, and σ_α is the total cross section, computed with the same matrix element. The momenta p_j of any invisible particles, such as neutrinos, are integrated over the available phase space. The combined logarithmic likelihood for a sample of N events approximately converges to a χ^2 distribution:

$$\chi^2 = -2 \ln(\mathcal{L}) = -2 \sum_{n=1}^N \ln \mathcal{P}(\mathbf{p}_{n,i}^{\text{vis}}|\alpha), \quad (2)$$

where $\mathbf{p}_{n,i}^{\text{vis}}$ are the measured momenta of the n th event.

By searching for the maximum of the likelihood, one can discriminate between several models and/or determine the parameters of a given model. The method is particularly powerful for the measurement of processes with low event yield and/or unreconstructible event kinematics due to the presence of invisible particles in the final state. Typical examples

are top quark physics at the Tevatron [6–8], Higgs searches [9, 10], and the production of dark matter particles at the LHC [11, 12].

This letter reports on the application of the MEM to the process $pp \rightarrow jjW^+W^+ \rightarrow jj\ell^+\ell'^+\nu_\ell\nu_{\ell'}$, where $\ell^{(\prime)} = e, \mu$ and j denotes a light quark jet. While this channel has a rather small cross section, due to the restriction to only positive charge and leptonic decay channels of the W bosons, it has the advantage of being experimentally clean and having low background. As a result, its sensitivity can be competitive with other vector boson scattering channels [3, 4]. An analysis of the W^+W^- channel, which has a larger signal rate, with the MEM is left for a future publication.

For the likelihood calculation and the cross-section normalization in eq. (1), the complete set of tree-level diagrams for the partonic processes $q\bar{q} \rightarrow q'\bar{q}'W^+W^+ \rightarrow q'\bar{q}'\ell^+\ell'^+\nu_\ell\nu_{\ell'}$ ($q, q' = u, d, s, c$) have been included, *i. e.* all diagrams with on-shell intermediate W bosons. Besides the contribution from longitudinal W^+W^+ scattering, this set also includes the irreducible background from all other diagrams leading to the same final state, $q'\bar{q}'W^+W^+$. It has been shown that the difference between considering only these diagrams and considering the full process $q\bar{q} \rightarrow q'\bar{q}'\ell^+\ell'^+\nu_\ell\nu_{\ell'}$, including off-shell and t-channel W exchange, is negligible for high energy WW scattering [4]. The analysis is performed at the parton-level—but note that the inclusion of transfer functions for jet smearing and initial-state radiation is conceptually straightforward [6, 7, 13] (see also [10]), although it substantially increases the computing time.

Signal events are defined through a set of preselection cuts:

$$\begin{aligned}
p_{T,\ell} &> 20 \text{ GeV}, & |\eta_\ell| &< 2.5, \\
p_{T,j} &> 30 \text{ GeV}, & |\eta_j| &< 5, & \Delta R_{jj,\ell j,\ell\ell} &> 0.4 \\
|\eta_{j_1} - \eta_{j_2}| &> 4, & |\eta_j| &> 1, & m_{j_1 j_2} &> 100 \text{ GeV}, \\
m_{\ell j} &> 190 \text{ GeV}.
\end{aligned} \tag{3}$$

Here $p_{T,i}$ and η_i are the transverse momentum and pseudorapidity, respectively, of a final-state object $i = \ell, j$; m_{ij} is the invariant mass of the two objects i and j ; and $\Delta R_{ij} \equiv \sqrt{(\eta_i - \eta_j)^2 + (\phi_i - \phi_j)^2}$ quantifies the separation of two objects in the plane of pseudorapidity and azimuthal angle. The first two lines in eq. (3) describe the general detector acceptance and object isolation cuts. The third line identifies the typical vector boson fusion topology, where the two jets are expected to go in the forward and backward directions, respectively². The last line removes background from $t\bar{t}$ production, which can produce an apparent same-sign lepton signal due to the small, but non-negligible, probability for lepton sign misidentification in the detector [4]. The invariant mass of a lepton-jet pair originating from top quark decay is bounded from above by the top mass m_t , so the requirement that the invariant mass of any lepton and jet is sufficiently larger than m_t eliminates that background, while about 25% of the signal events are retained.

The determination of the MEM weights (*i. e.* the numerator in eq. (1)) and cross section normalization factors (denominator in eq. (1)) has been carried out with a specialized private

²These cuts are kept relatively loose since their primary purpose is to reduce the number of input event to a reasonable amount. Further improvement of the signal significance is left to the MEM.

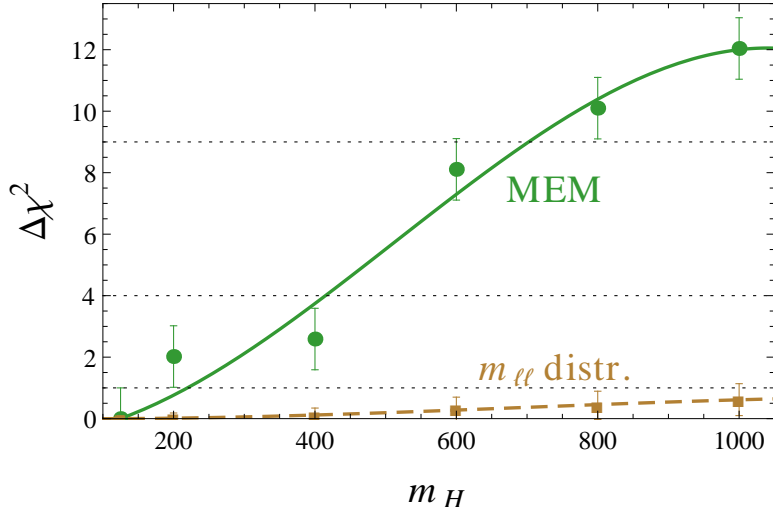


Figure 1: Statistical discrimination between different SM Higgs masses from analyzing the process $pp \rightarrow jjW^+W^+ \rightarrow jj\ell^+\ell'^+\nu_\ell\nu_{\ell'}$ using the MEM (circles) vs. the di-lepton mass distribution (squares). The results are based on 100 events simulated for $m_{H,\text{ref}} = 125$ GeV and $\sqrt{s} = 14$ TeV. The error bars indicate the uncertainty from the event statistics.

code³, using diagrams generated with FEYNARTS 3.3 [14]. As a cross-check, the results have been cross-checked against MADGRAPH/MADEVENT 5 [15] and MADWEIGHT 2.5 [12] and good agreement has been found⁴. MADEVENT has also been used for the generation of the simulated “experimental” events that are fed into the MEM fit. Throughout this paper, the “experimental” events sample is based on the SM with $m_{H,\text{ref}} = 125$ GeV. The cuts (3) have been consistently applied both to the event generation and weight normalization.

In the following the analysis of the process $pp \rightarrow jjW^+W^+ \rightarrow jj\ell^+\ell'^+\nu_\ell\nu_{\ell'}$ with the MEM is presented for three characteristic models: the Standard Model (SM), the Two Higgs Doublet Model (THDM), and the Strongly Interacting Light Higgs (SILH) Model.

SM: For $m_H = 125$ GeV, the signal cross section for $\sqrt{s} = 14$ TeV after the preselection cuts is 0.590 fb, resulting in a signal yield of 100 events with an integrated luminosity of 170 fb^{-1} . Assuming this number of signal events, the results of the MEM likelihood fit are shown in Fig. 1. Specifically, if one wants to test whether the unitarization of WW scattering is facilitated by a light Higgs boson with $m_H = 125$ GeV or a heavy Higgs boson with $m_H = 1000$ GeV, these two hypotheses could be distinguished with a statistical significance of more than three standard deviations.

For comparison, Fig. 1 shows the statistical discrimination obtained from analyzing the $m_{\ell\ell}$ distribution as suggested *e.g.* in Ref. [3]. When using two bins in the range $m_{\ell\ell} \in [0, 1000]$ GeV and a sample of 100 events, the significance stays below one standard deviation

³The code is available upon request from the authors.

⁴It was difficult to reach the required precision for the cross section values with MADGRAPH/MADEVENT within a reasonable amount of computing time, so the results presented here are based on our private code.

for Higgs masses up to 1 TeV. With larger numbers of bins the discriminative power is even lower.

Of course, in light of electroweak precision tests and the evidence for a 125-GeV scalar at LHC [1], the SM with a heavy Higgs boson is effectively excluded. Nevertheless it is illustrative to discuss this scenario as a simple example that tangibly highlights the difference between the MEM and a traditional analysis strategy.

THDM: A more realistic scenario is given by the THDM with a light CP-even Higgs boson (h^0) of mass $m_h = 125$ GeV, which explains the observed Higgs signal, and a heavy CP-even Higgs (H^0) with unconstrained mass m_H [16]. Assuming CP conservation, the two physical states h^0 and H^0 are mixtures of the CP-even components of the two Higgs doublets, H_1^0 and H_2^0 :

$$\begin{aligned} h^0 &= \cos \alpha H_1^0 - \sin \alpha H_2^0, \\ H^0 &= \sin \alpha H_1^0 + \cos \alpha H_2^0. \end{aligned} \tag{4}$$

Denoting the ratio of the vacuum expectation values by $\langle H_2^0 \rangle / \langle H_1^0 \rangle = \tan \beta$, the Higgs- W - W couplings read

$$\begin{aligned} \frac{g(h^0 WW)_{\text{THDM}}}{g(HWW)_{\text{SM}}} &= \cos(\beta - \alpha) \equiv \cos \xi, \\ \frac{g(H^0 WW)_{\text{THDM}}}{g(HWW)_{\text{SM}}} &= \sin(\beta - \alpha) \equiv \sin \xi, \end{aligned} \tag{5}$$

where $g(HWW)_{\text{SM}}$ is the HWW coupling in the SM. If $\xi \equiv \beta - \alpha$ is non-negligible, both h^0 and H^0 play a role in the unitarization of WW scattering. As shown in Fig. 2, the interplay of the two Higgs bosons in this process can be tested experimentally with the help of the MEM. In particular, a sample of just 100 events will be sufficient to rule out the parameter region with large values of $\xi \gtrsim \pi/4$ and $m_{H^0} \gtrsim 600$ GeV at about 90% confidence level [assuming the data agrees with the SM].

SILH: The SILH paradigm encompasses a class of models with strong dynamics at the scale $\Lambda \sim 4\pi f > 1$ TeV and a light composite Higgs boson, which is a pseudo-Goldstone boson of some global symmetry [17]. As a low-energy effective theory, it contains a light Higgs whose coupling to W and Z are modified by a factor $1/\sqrt{1 - cv^2/f^2}$, where c is a $\mathcal{O}(1)$ number. As a result, unitarization of high energy vector boson scattering is not achieved by the light Higgs alone, but requires the presence of additional heavy scalar and vector resonances, which emerge from the strong sector. Here it is assumed that these resonance are beyond the reach of the LHC, so that the only observable effect are the modified hWW and hZZ couplings⁵, which is equivalent to the limit $m_{H^0} \rightarrow \infty$ of the THDM.

Similar to the previous examples, the deformation parameter cv^2/f^2 can be constrained by analyzing high energy W^+W^+ through the process $pp \rightarrow jjW^+W^+ \rightarrow jj\ell^+\ell'^+\nu_\ell\nu_{\ell'}$. The output of the MEM as a function of this parameter is shown in Fig. 3, together with the

⁵The explicit inclusion of the heavy resonances in the MEM does not pose any conceptual problem, but due to the substantial amount of computing time involved this is left for future work.

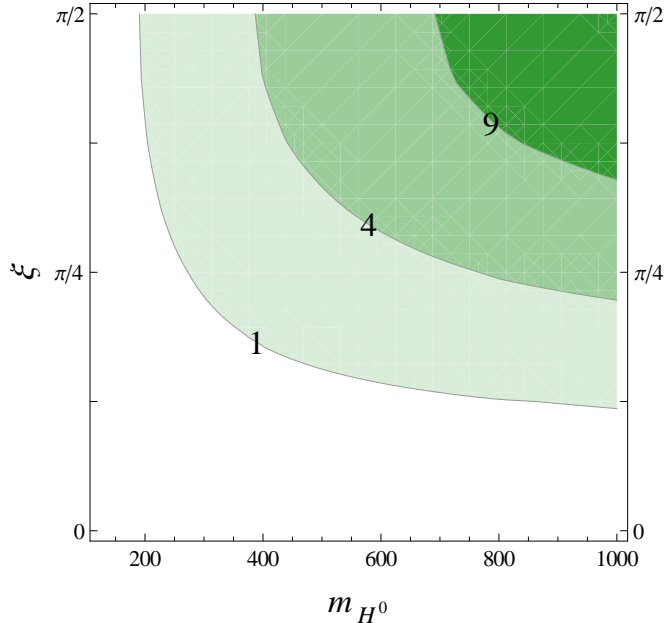


Figure 2: Projected constraints on the THDM from the MEM analysis of the process $pp \rightarrow jjW^+W^+ \rightarrow jj\ell^+\ell'^+\nu_\ell\nu_{\ell'}$, as function of the heavy Higgs mass m_{H^0} and the mixing angle ξ (the light Higgs mass is fixed to $m_{h^0} = 125$ GeV). The contour lines indicate $\Delta\chi^2 = 1, 4, 9$. The results are based on 100 events simulated for $\xi = 0$ and $\sqrt{s} = 14$ TeV.

results obtained from analyzing the $m_{\ell\ell}$ distribution. It has been checked that the latter are compatible with the numbers in Tab. 14 of Ref. [3] within statistical errors. As evident from the figure, the MEM leads to an improvement of the sensitivity by more than one standard deviation.

Conclusions: High energy vector boson scattering provides a unique window into the mechanism of electroweak symmetry breaking, but it is difficult to analyze experimentally at the LHC due to the small event yield. The Matrix Element Method (MEM), which is an automated likelihood technique incorporating all relevant event and theory information, significantly improves the sensitivity for this process as compared with traditional analysis methods. This had been demonstrated explicitly here for high energy W^+W^+ scattering. As concrete examples, the method has been applied to three characteristic examples, the Standard Model with variable Higgs mass, the Two Higgs Doublet Model, and the Strongly Interacting Light Higgs Model, but it can be adapted straightforwardly to other models of electroweak symmetry breaking by implementing the relevant matrix elements.

It is worth pointing out that the method does not rely on the observation of a resonance. In fact, for high energy same-sign WW scattering, the Higgs boson or any other unitarity-restoring particle contributes only in the t-channel. Consequently, the MEM will be useful even for a so-called “nightmare” scenario with very broad resonances [18].

The results presented here are based on a parton-level analysis. For a more realistic

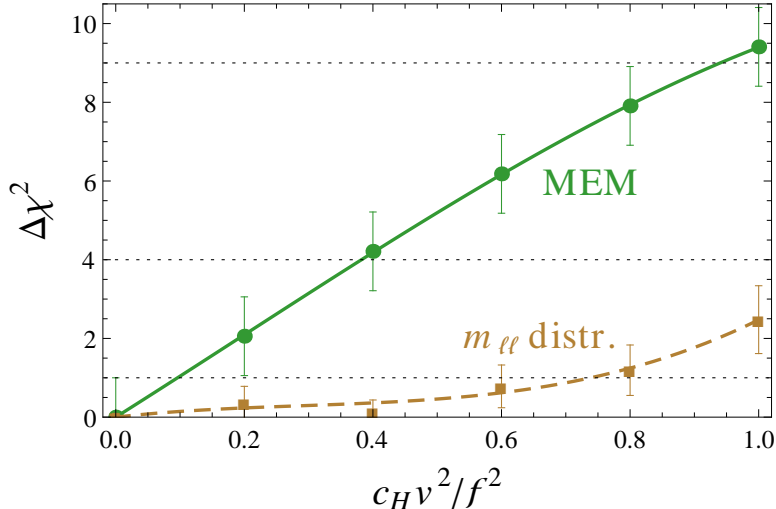


Figure 3: Statistical discrimination between different values of the deformation parameter $c v^2/f^2$ in SILH models from analyzing the process $pp \rightarrow jjW^+W^+ \rightarrow jj\ell^+\ell'^+\nu_\ell\nu_{\ell'}$ using the MEM (circles) vs. the di-lepton mass distribution (squares). The results are based on 100 events simulated for $m_{H,\text{ref}} = 125$ GeV, $c_H = 0$, and $\sqrt{s} = 14$ TeV. The error bars indicate the uncertainty from the event statistics.

picture, one needs to consider systematic uncertainties and detector effects. The largest systematic error is related to the measurement of the jet energy, which can be taken into account by incorporating jet smearing functions and by treating the overall jet energy scale as a free parameter in the fit [6]. While this leads to a substantial increase in computing time, the sensitivity of the MEM is not significantly reduced.

A potentially important reducible background arises from events in which a W boson (which decays to an electron or positron together with the corresponding neutrino) is produced with three associated jets, and one of the jets is incorrectly identified as an electron or positron. For reasonable values of the rate at which jets are incorrectly reconstructed as electrons ($\sim 10^{-4}$), a preliminary analysis suggests that the rate for this process may be $\sim 15\%$ of the signal rate. More exhaustive studies by the LHC detector collaborations are necessary for a precise determination of the significance of this background, though it can probably be reduced by imposing more stringent criteria in electron reconstruction.

Other systematic effects include next-to-leading order QCD corrections, which are small for vector boson fusion processes [19], and uncertainties in the quark and antiquark parton distribution functions (PDFs). While PDF errors for $WWjj$ production are already at the level of a few percent [20], the availability of substantial LHC data should reduce these errors further, due to a better understanding of the light quark flavor distribution in the relevant range of x , and different experimental systematics compared to deep inelastic scattering. Therefore it is expected that the effectiveness of the MEM will not be significantly reduced by systematic errors.

Acknowledgments: The authors would like to thank J. Alwall for helpful communications. AF gratefully acknowledges the warm hospitality at the Michigan Center for Theoretical Physics during part of this project. JG likewise thanks the Aspen Center for Physics (funded by NSF Grant #1066293) for their hospitality and the SLAC National Accelerator Laboratory for the use of computing resources. This work was partially supported by the National Science Foundation under grant PHY-1212635 and by the Department of Energy under grants DE-AC02-06CH11357, DE-FG02-91ER40684, and DE-FG02-97ER41029.

References

- [1] G. Aad *et al.* [ATLAS Collaboration], Phys. Lett. B **716**, 1 (2012); S. Chatrchyan *et al.* [CMS Collaboration], Phys. Lett. B **716**, 30 (2012).
- [2] M. J. Duncan, G. L. Kane and W. W. Repko, Nucl. Phys. B **272**, 517 (1986); D. A. Dicus and R. Vega, Phys. Rev. Lett. **57**, 1110 (1986); R. Kleiss and W. J. Stirling, Phys. Lett. B **200**, 193 (1988); V. D. Barger, K. Cheung, T. Han and R. J. N. Phillips, Phys. Rev. D **42**, 3052 (1990); U. Baur and E. W. N. Glover, Phys. Lett. B **252**, 683 (1990); D. A. Dicus, J. F. Gunion and R. Vega, Phys. Lett. B **258**, 475 (1991); D. A. Dicus, J. F. Gunion, L. H. Orr and R. Vega, Nucl. Phys. B **377**, 31 (1992); J. Bagger *et al.*, Phys. Rev. D **49**, 1246 (1994) and D **52**, 3878 (1995); K. Iordanidis and D. Zeppenfeld, Phys. Rev. D **57**, 3072 (1998); J. M. Butterworth, B. E. Cox and J. R. Forshaw, Phys. Rev. D **65**, 096014 (2002); A. Alboteanu, W. Kilian and J. Reuter, JHEP **0811**, 010 (2008); C. Englert, B. Jäger, M. Worek and D. Zeppenfeld, Phys. Rev. D **80**, 035027 (2009); A. Ballestrero, G. Bevilacqua and E. Maina, JHEP **0905**, 015 (2009); A. Ballestrero, G. Bevilacqua, D. B. Franzosi and E. Maina, JHEP **0911**, 126 (2009); G. Aad *et al.* [ATLAS Collaboration], arXiv:0901.0512 [hep-ex].
- [3] A. Ballestrero, D. B. Franzosi and E. Maina, JHEP **1106**, 013 (2011).
- [4] K. Doroba *et al.*, Phys. Rev. D **86**, 036011 (2012).
- [5] K. Kondo, J. Phys. Soc. Jap. **57**, 4126 (1988) and **60**, 836 (1991); R. H. Dalitz and G. R. Goldstein, Phys. Rev. D **45**, 1531 (1992).
- [6] B. Abbott *et al.* [DØ Collaboration], Phys. Rev. D **60**, 052001 (1999); V. M. Abazov *et al.* [DØ Collaboration], Nature **429**, 638 (2004).
- [7] A. Abulencia *et al.* [CDF Collaboration], Phys. Rev. D **75**, 031105 (2007); F. Fiedler, A. Grohsjean, P. Haefner and P. Schieferdecker, Nucl. Instrum. Meth. A **624**, 203 (2010).
- [8] V. M. Abazov *et al.* [DØ Collaboration], Phys. Rev. D **78**, 012005 (2008); T. Aaltonen *et al.* [CDF Collaboration], Phys. Rev. Lett. **101**, 252001 (2008).
- [9] S.-C. Hsu *et al.* [CDF Collaboration], CDF note 8774 (2007); T. Aaltonen *et al.* [CDF Collaboration], Phys. Rev. D **80**, 071101 (2009); J. Therhaag, Diplom thesis, University of Bonn, BONN-IB-2009-03 (2009); D. E. Soper and M. Spannowsky, Phys. Rev. D **84**,

- 074002 (2011); J. S. Gainer, K. Kumar, I. Low and R. Vega-Morales, JHEP **1111**, 027 (2011); J. S. Gainer, W.-Y. Keung, I. Low and P. Schwaller, Phys. Rev. D **86**, 033010 (2012); P. Avery *et al.*, Phys. Rev. D **87**, 055006 (2013); J. R. Andersen, C. Englert and M. Spannowsky, Phys. Rev. D **87**, 015019 (2013).
- [10] J. M. Campbell, W. T. Giele and C. Williams, JHEP **1211**, 043 (2012).
- [11] J. Alwall, A. Freitas and O. Mattelaer, AIP Conf. Proc. **1200**, 442 (2010); C.-Y. Chen and A. Freitas, JHEP **1102**, 002 (2011).
- [12] P. Artoisenet, V. Lemaître, F. Maltoni and O. Mattelaer, JHEP **1012**, 068 (2010).
- [13] J. Alwall, A. Freitas and O. Mattelaer, Phys. Rev. D **83**, 074010 (2011).
- [14] T. Hahn, Comput. Phys. Commun. **140**, 418 (2001).
- [15] J. Alwall, M. Herquet, F. Maltoni, O. Mattelaer and T. Stelzer, JHEP **1106**, 128 (2011).
- [16] W. Altmannshofer, S. Gori and G. D. Kribs, Phys. Rev. D **86**, 115009 (2012); S. Chang, S. K. Kang, J.-P. Lee, K. Y. Lee, S. C. Park and J. Song, JHEP **1305**, 075 (2013); Y. Bai, V. Barger, L. L. Everett and G. Shaughnessy, arXiv:1210.4922 [hep-ph].
- [17] G. F. Giudice, C. Grojean, A. Pomarol and R. Rattazzi, JHEP **0706**, 045 (2007).
- [18] A. Falkowski, C. Grojean, A. Kaminska, S. Pokorski and A. Weiler, JHEP **1111**, 028 (2011).
- [19] B. Jäger, C. Oleari and D. Zeppenfeld, Phys. Rev. D **80**, 034022 (2009).
- [20] P. Bolzoni, F. Maltoni, S.-O. Moch and M. Zaro, Phys. Rev. D **85**, 035002 (2012).